# Experimental optimum design and luminescence properties of $NaY(Gd)(MoO_4)_2:Er^{3+}$ phosphors*

Jia-Shi Sun(孙佳石)†, Sai Xu(徐赛)‡, Shu-Wei Li(李树伟), Lin-Lin Shi(石琳琳), Zi-Hui Zhai(翟梓会), and Bao-Jiu Chen(陈宝玖)

*Department of Physics, Dalian Maritime University, Dalian* 116026, *China*

(Received 11 December 2015; revised manuscript received 4 February 2016; published online 20 April 2016)

Three-factor orthogonal design (OD) of $Er^{3+}/Gd^{3+}/T$ (calcination temperature) is used to optimize the luminescent intensity of $NaY(Gd)(MoO_4)_2:Er^{3+}$ phosphor. Firstly, the uniform design (UD) is introduced to explore the doping concentration range of $Er^{3+}/Gd^{3+}$. Then OD and range analysis are performed based on the results of UD to obtain the primary and secondary sequence and the best combination of $Er^{3+}$, $Gd^{3+}$, and T within the experimental range. The optimum sample is prepared by the high temperature solid state method. Photoluminescence excitation and emission spectra of the optimum sample are detected. The intense green emissions (530 nm and 550 nm) are observed which originate from $Er^{3+}$ $^2H_{11/2} \rightarrow {}^4I_{15/2}$ and $^4S_{3/2} \rightarrow {}^4I_{15/2}$, respectively. Thermal effect is investigated in the optimum $NaY(Gd^{3+})(MoO_4)_2:Er^{3+}$ phosphors, and the green emission intensity decreases as temperature increases.

**Keywords:** orthogonal design (OD), uniform design (UD), $NaY(Gd)(MoO_4)_2:Er^{3+}$, luminescent intensity

**PACS:** 33.50.Dq, 02.10.Yn, 02.90.+p, 33.20.Kf **DOI:** 10.1088/1674-1056/25/6/063301

## 1. Introduction

In recent years, trivalent rare earth ions have attracted much attention, due to their substantial advantages such as sharp emission lines, high color purity, strong capacity of light absorption, and high photoelectric conversion efficiency, etc.[1–3] Among numerous rare earth ions, $Er^{3+}$ ions which act as activators for host material have been extensively studied and the research is concentrated on their high luminescent efficiencies. Currently, researchers pay more attention to $Er^{3+}$ doped phosphors due to their plentiful energy levels and more pumping ways of up-conversion luminescence.[4–6] Though $Er^{3+}$ has received great attention for the past few years, the relatively low absorption cross section of $Er^{3+}$ ions leads to very poor luminescent efficiency.[7,8] On the other hand, $Gd^{3+}$ is a special lanthanide element which can act as a good activator as well as a good sensitizer due to its half full 4f shell which can absorb and transfer energy effectively between trivalent rare earth ions. Moreover, $Gd^{3+}$ with simple level structure and long excited state lifetime can easily match with $Er^{3+}$ energy level $Gd^{3+}$ and $Er^{3+}$ co-doped materials can improve the luminescence efficiency.[9–11] Additionally molybdates have aroused considerable interest as a momentous host material possessing some specific properties to accommodate optically active rare-earth ions.[12,13] Molybdates can availably absorb blue or purple LED light and transfer to the rare earth ions. Studies on molybdates mainly focus on $AX(MoO_4)_2$ with a similar scheelite structure which has high randomness to broaden the spectrum inhomogeneously, augments the excited absorption cross section and weakens laser thermal effect.[14]

Luminescence intensity is a critical index to evaluate the luminescence performance of phosphor. The primary problem is how to figure out the optimum synthesis parameters of the phosphors in the experimental domain. Orthogonal design (OD) is the most prevalent fractional factorial design using orthogonal table to design scheme, choose the most effective test sites without losing the main information in the experimental range, which can significantly reduce the number of experimental runs.[15,16] The key to a successful experiment is the appropriate factors and the related variable span. In our experiment several factors will affect the luminescence intensity of luminescence material, and we consider three factors: the doping concentrations of $Er^{3+}$ and $Gd^{3+}$, and synthesized temperature $T$ at the green emission intensity of $NaY(Gd^{3+})(MoO_4)_2:Er^{3+}$ phosphors.

In order to obtain $NaY(Gd^{3+})(MoO_4)_2:Er^{3+}$ phosphors with a maximum green emission intensity, the method of UD[17–20] is primarily employed to quickly narrow down the scope of factors and achieve the probable concentration ranges of $Er^{3+}$ and $Gd^{3+}$, and then OD and range analysis are used

*Project supported by Education Reform Fund of Dalian Maritime University, China (Grant No. 2015Y37), the Natural Science Foundation of Liaoning Province, China (Grant Nos. 2015020190 and 2014025010), the Open Fund of the State Key Laboratory on Integrated Optoelectronics, China (Grant No. IOSKL2015KF27), and the Fundamental Research Funds for the Central Universities, China (Grant No. 3132016121).

†Corresponding author. E-mail: sunjs@dlmu.edu.cn

‡Corresponding author. E-mail: xsjlu@126.com

© 2016 Chinese Physical Society and IOP Publishing Ltd 

to ascertain the optimum combinations of $Er^{3+}$, $Gd^{3+}$, and $T$. The OD is proved to be a fairly straightforward and cost-effective optimization strategy that can be employed to assign test factors in a series of experimental trials.[21] It is worth noting that this method emphasizes the global optimization throughout the whole process of experimental design and datum analysis. The optimum $NaY(Gd^{3+})(MoO_4)_2:Er^{3+}$ phosphor sample is synthesized by the high temperature solid state method. Photoluminescence excitation (PLE) and emission (PL) spectra are measured. The green emission integrated intensity of $NaY(Gd^{3+})(MoO_4)_2:Er^{3+}$ phosphor under the optimal condition is in good agreement with the theoretical optimum result. In addition, the temperature-quenching mechanism of the optimum sample is also analyzed.

## 2. Experiment

### 2.1. UD and OD

Reagent grade $Gd_2O_3$, $Er_2O_3$, $Y_2O_3$, $MoO_3$, and $Na_2CO_3$ were used while $NH_4HF_2$ was used as a flux. The composition of the compound used was $Na_2CO_3$–$z_1Gd_2O_3$–$z_2Er_2O_3$–$(1-z_1-z_2)Y_2O_3$–$4MoO_3$, where $z_1$ varies from 60 mol% to 90 mol% and $z_2$ from 5.5 mol% to 8.5 mol% based on UD result as shown in Table 1. We can intuitively infer from the strongest green luminescent intensity listed in the ninth line that the rare earth ion domain is $Er^{3+}$[5.5%,8.5%]*$Gd^{3+}$[60%,90%]. Moreover $T$ ranges from 700 °C to 1100 °C.

**Table 1.** Design and result of UD.

| $T = 800$ °C | $C$ ($Gd^{3+}$) (0–100) mol% | $C$ ($Er^{3+}$) (0–15) mol% | $Y$/a.u. |
|---|---|---|---|
| 1 | 1 (0) | 8 (11.69) | 5264 |
| 2 | 2 (11) | 4 (5.01) | 4153 |
| 3 | 3 (22) | 7 (10.02) | 6312 |
| 4 | 4 (33) | 3 (3.34) | 7701 |
| 5 | 5 (44) | 10 (15) | 4480 |
| 6 | 6 (55) | 6 (8.35) | 7071 |
| 7 | 7 (67) | 2 (1.67) | 8493 |
| 8 | 8 (78) | 9 (13.36) | 3592 |
| 9 | 9 (89) | 5 (6.68) | 8664 |
| 10 | 10 (100) | 1 (0) | – |

The orthogonal table $L_{16}(4^5)$ was used in the experiment, and four levels were set for each factor. Based on the investigation factors and the corresponding levels, the combination of doping concentrations and $T$ are arranged by orthogonal table shown in Table 2. Here $x_1$, $x_2$, and $x_3$ are factorial code values corresponding to actual values of percentage concentration of $Gd^{3+}$ ($z_1$), percentage concentration of $Er^{3+}$ ($z_2$), and $T$ ($z_3$) respectively.

**Table 2.** Design and results of $L_{16}(4^5)$ OD.

| | $A$ (Gd) $x_1(z_1)$/mol% | $B$ (Er) $x_2(z_2)$/mol% | $C$ ($T$) $x_3(z_3)$/°C | $Y$ Intensity/a.u. |
|---|---|---|---|---|
| 1 | 1 (60) | 1 (5.5) | 1 (700) | 5724 |
| 2 | 1 (60) | 2 (6.5) | 2 (833) | 7917 |
| 3 | 1 (60) | 3 (7.5) | 3 (966) | 8151 |
| 4 | 1 (60) | 4 (8.5) | 4 (1100) | 9038 |
| 5 | 2 (70) | 1 (5.5) | 4 (1100) | 13113 |
| 6 | 2 (70) | 2 (6.5) | 3 (966) | 9116 |
| 7 | 2 (70) | 3 (7.5) | 2 (833) | 6114 |
| 8 | 2 (70) | 4 (8.5) | 1 (700) | 5900 |
| 9 | 3 (80) | 1 (5.5) | 2 (833) | 8673 |
| 10 | 3 (80) | 2 (6.5) | 1 (700) | 5760 |
| 11 | 3 (80) | 3 (7.5) | 4 (1100) | 10337 |
| 12 | 3 (80) | 4 (8.5) | 3 (966) | 8061 |
| 13 | 4 (90) | 1 (5.5) | 3 (966) | 10923 |
| 14 | 4 (90) | 2 (6.5) | 4 (1100) | 10827 |
| 15 | 4 (90) | 3 (7.5) | 1 (700) | 4383 |
| 16 | 4 (90) | 4 (8.5) | 2 (833) | 6728 |
| $K_1$ | 7708 | 9608 | 5442 | – |
| $K_2$ | 8561 | 8405 | 7358 | – |
| $K_3$ | 8207 | 7246 | 9063 | – |
| $K_4$ | 8215 | 7432 | 10829 | – |
| R | 853 | 2362 | 5387 | – |

### 2.2. Sample preparation

The traditional high-temperature solid-state method was used for synthesizing the phosphors. The starting materials were accurately weighed according to the certain doping concentrations assigned through orthogonal design. These weighed powders should be fully ground to ensure a homogeneous blend and then the mixtures were poured into an alumina crucible. Afterwards, the mixture powders were calcined at different temperatures (from 700 °C to 1100 °C) for 4 h. Finally the wanted phosphors were obtained by grinding the bulk materials into powders.

### 2.3. Sample measurements

The crystalline structure of the optimum phosphor was characterized by x-ray diffraction (XRD) (Shimadzu XRD-6000 diffractometer with Cu $K\alpha_1$ radiation source radiation ($\lambda = 0.15406$ nm)). The scanning region of $2\theta$ angles was from 10 °C to 70 °C in scanning step of 0.02°. PLE and PL spectra of the samples were measured by a Hitachi F-4600 fluorescence spectrometer equipped with a 150-W Xenon lamp.

## 3. Results and discussion

### 3.1. Photoluminescence properties

PLE and PL spectra for all the prepared samples are measured under the same experimental conditions. The integrated intensities denoted as $Y$ value for the green emission are calculated and shown in Table 2. Figure 1 shows the excitation spectrum of $NaY(Gd^{3+})(MoO_4)_2:Er^{3+}$ phosphor monitored at 552 nm. It can be clearly seen that there is a broad intense band

at 315 nm and a narrow peak with a maximum at 380 nm as well as some other weak lines in the wavelength region. In accordance with Refs. [22] and [23] the broad band at 315 nm could be assigned to the O–Mo ligand-to-metal charge-transfer state from $MoO_4^{2-}$ unit in the $NaY_2(MoO_4)_2$ host lattice. In the excitation spectrum of $NaY(Gd^{3+})(MoO_4)_2$:$Er^{3+}$ phosphor, the broad absorption band from 250 nm to 350 nm is observed, which does not originate from $Er^{3+}$ but from $MoO_4^{2-}$ group. Thus, we think there exists an energy transfer process between $MoO_4^{2-}$ group and $Er^{3+}$. In this process, $MoO_4^{2-}$ group acts as an energy transfer donor, and $Er^{3+}$ ion acts as an acceptor. The other excitation bands peaking at around 365.2, 378.4, 407.2, 451.4, 488.2, and 521.4 nm are derived from $Er^{3+}$ $^4I_{15/2} \rightarrow {}^2K_{15/2}$, $^4I_{15/2} \rightarrow {}^4G_{11/2}$, $^4I_{15/2} \rightarrow {}^2H_{9/2}$, $^4I_{15/2} \rightarrow {}^4F_{3/2}$, $^4I_{15/2} \rightarrow {}^4F_{5/2}$, and $^4I_{15/2} \rightarrow {}^4F_{7/2}$, respectively. The emission spectrum of $Er^{3+}$ is obtained under the 380 nm excitation. From Fig. 2 the green emission bands peaking at around 530 nm and 550 nm corresponding to the transitions from the excited states $^2H_{11/2}$ and $^4S_{3/2}$ to the ground state $4I_{15/2}$ are observed.[24] Otherwise, under the excitation of 380 nm ($\lambda_{ex} = 380$ nm) each emission peak is due to $Er^{3+}$ characteristic emission spectrum and it has no $Gd^{3+}$ characteristic emission spectrum. Therefore the luminescence of $NaY(Gd^{3+})(MoO_4)_2$:$Er^{3+}$ phosphor is not induced by $Gd^{3+}$ but $Er^{3+}$.

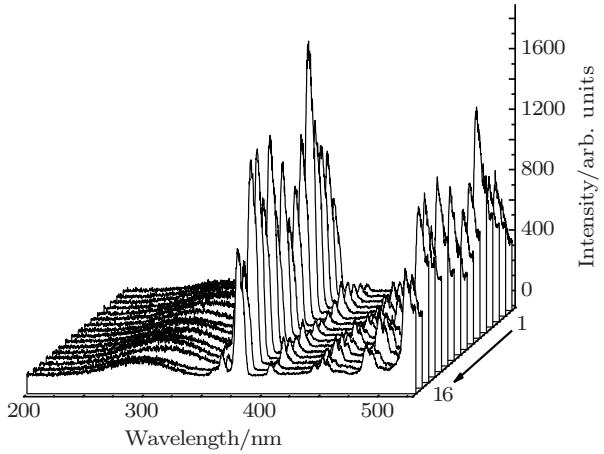



**Fig. 1.** Excitation spectrum of $NaY(Gd^{3+})(MoO_4)_2$:$Er^{3+}$ phosphor.

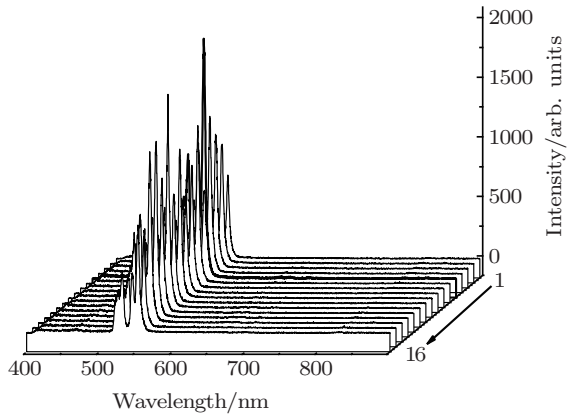



**Fig. 2.** Emission spectrum of $NaY(Gd^{3+})(MoO_4)_2$:$Er^{3+}$ phosphor.

### 3.2. Result analysis of OD by range analysis

A reliable experimental result largely depends on appropriate analysis methods; moreover optimal design analysis is an indispensable component of orthogonal design. Even the best experimental design cannot struggle to meet the requirements for its experimental goals without appropriate optimal analysis methods. We have employed several analysis methods in previous work[25] such as variance analysis and GA (Genetic Algorithm). However, range analysis[26–28] has been proved to be a visual and vivid method through simple calculation and judgment, which can optimize the experimental results: preliminary and secondary factors, optimal levels and optimum combination. Range analysis aims to illustrate the significant levels of various influencing factors on the green light luminescence intensity and ascertain the best combination of $z_1$, $z_2$, and $z_3$. Summarized in Table 2 is the statistic analysis of the green light luminescence intensity of three factors of orthogonal design.

The $K$ value for each level of a parameter is the average of four values shown in the last column in Table 2. We can determine the optimum level of each factor and further obtain the optimum combination according to the $K$ value. The range value ($R$) for each factor reflects the indicator range with corresponding factor change, which equals the minimum of $K$ subtracted from a maximum. Normally, the larger the $R$ value, the greater the influence on the result. According to the results of range analysis, the order of significance levels is $z_3 > z_2 > z_1$, for the green luminescence intensity. In other words, the calcination temperature ($T$) has a greater influence on the green luminescent intensity of $NaY(Gd)(MoO_4)_2$:$Er^{3+}$ phosphors than the other two factors since the phosphors may present different luminescence performances at different calcination temperatures. In general the luminescence intensity increases with the rising of the calcination temperature within certain limits on account of high temperature contribution to well crystallizing. The optimal combination $A_2B_1C_4$ is also obtained from Table 2. Therefore, it could be concluded that the optimum conditions to synthesize $NaY(Gd^{3+})(MoO_4)_2$:$Er^{3+}$ phosphors are that $Gd^{3+}$ concentration is 70%, $Er^{3+}$ concentration is 5.5% and calcination temperature is 1100 °C in our experiment. Just as it is, the fifth sample in Table 2 is the sample under the optimum combination, which shows the maximum green luminescent intensity.

### 3.3. Structural characterization

Figure 3 shows the XRD pattern of the optimal sample of $NaY(Gd^{3+})(MoO_4)_2$:$Er^{3+}$ phosphors doped with 70 mol% $Gd^{3+}$/5.5 mol% $Er^{3+}$ calcined at 1100 °C and also the XRD pattern from the standard card of $NaY(MoO_4)_2$ for compari-

son. It can be found that diffraction peaks are in accordance with those obtained from JCPDs files of $NaY(MoO_4)_2$.

The position of the main peak has a gradual shift towards the lower degree, which indicates that $Gd^{3+}$ doping is mainly in the way of replacing $Y^{3+}$ rather than $Mo^{6+}$. If $Gd^{3+}$ replaces the site of $Mo^{6+}$, the characteristics of crystal will change a lot due to the large radius gap between the two ions. Reversely, the radius, valence and electronegativity of $Gd^{3+}$ ion are close to those of $Y^{3+}$ ion, so replacing can easily be realized. This fact indicates that $NaY(Gd^{3+})(MoO_4)_2$:$Er^{3+}$ phosphors can be produced by the traditional high temperature solid state reaction method and that the $NaY(Gd^{3+})(MoO_4)_2$:$Er^{3+}$ phosphors doping at the present level does not cause any remarkable change in crystal structure.

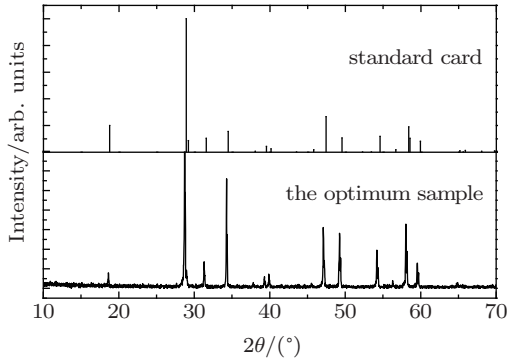



**Fig. 3.** Comparison of XRD of the optimal sample with that from standard card of $NaY(MoO_4)_2$.

### 3.4. Thermal quenching properties of down-conversion luminescence

In recent years, many researchers have studied the thermal stability of phosphors. Figure 4 shows the thermal quenching of the down-conversion emission spectra at different temperatures from 300 K to 723 K. For understanding the thermal quenching mechanism of the optimal $NaY(Gd^{3+})(MoO_4)_2$:$Er^{3+}$ phosphors, when the thermal excitation rate is considered, the luminescence intensities of $^4S_{3/2}$ and $^2H_{1/2}$ levels can be written as

$$I_S = \alpha \frac{A_r}{A_r + W_{et} + W_{nr}(0)\left[1-\exp\left(-\frac{h\nu}{kT}\right)\right]^{-p}} \times \frac{1}{1+C\exp\left(-\frac{\Delta E}{kT}\right)}, \quad (1)$$

$$I_H = \alpha \frac{A_r}{A_r + W_{et} + W_{nr}(0)\left[1-\exp\left(-\frac{h\nu}{kT}\right)\right]^{-p}} \times \frac{C\exp\left(-\frac{\Delta E}{kT}\right)}{1+C\exp\left(-\frac{\Delta E}{kT}\right)}, \quad (2)$$

where $\alpha$ is a coefficient, $A_r$ presents the radiative transition, $W_{et}$ is the energy transfer rate from the luminescence level $^4S_{3/2}$, and $W_{nr}(0)$ is the initial nonradiative relaxation rate at temperature close to zero, $\nu$ is the effective photon frequency, $h$ is the Planck's constant, $k$ is the Boltzmann's constant, and $p$ is the effective phonon mode number, and $\Delta E$ is the energy difference between $^2H_{11/2}$ and $^4S_{3/2}$ levels.[29] The two green emissions' integrated intensities at various temperatures are fitted by Eqs. (1) and (2), the curves in Fig. 5 show the fitting results.

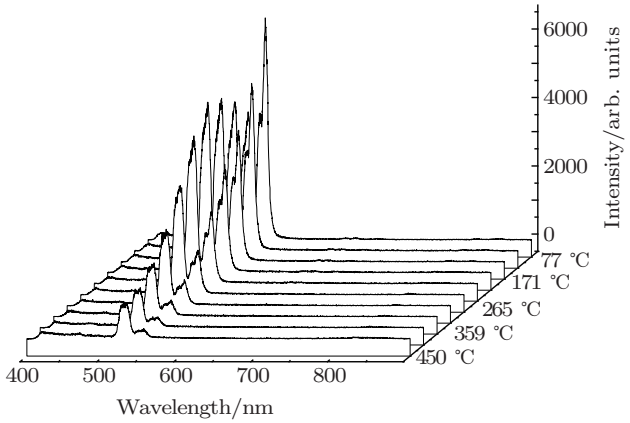



**Fig. 4.** Emission spectra of the optimal $NaY(Gd^{3+})(MoO_4)_2$:$Er^{3+}$ phosphor at different temperatures.

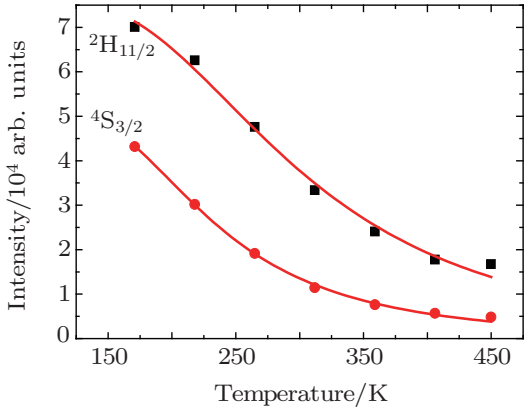



**Fig. 5.** (color online) Dependences of luminescence intensities (■ for $^2H_{11/2}$–$^4I_{15/2}$ and • for $^4S_{3/2}$–$^4I_{15/2}$) on temperature.

As the energy difference between $^2H_{11/2}$ and $^4S_{3/2}$ levels is small, the green emission integrated intensities at various temperatures can be fitted by the following equation according to classical thermal quenching theory:[30,31]

$$I(T) = \frac{I_0}{1+A\exp(-\Delta E/kT)}, \quad (3)$$

where $I$ represents the initial intensity, $I(T)$ represents the intensity at a certain temperature $T$, $A$ refers to the frequency factor of radioactive transition, $k$ is Boltzmann's constant, and $\Delta E$ is activation energy of thermal quenching. In Eq. (3), $I$, $A$, and $\Delta E$ act as free parameters. The value of activation energy $\Delta E$ exhibited in Fig. 6 is fitted as 0.41 eV by using commodity software Origin.

The degradation of green emission intensity originating from temperature increasing is half the initial intensity at 550 K, thus the quenching temperature ($T_{50}$) is confirmed to be 550 K. The temperature stability of the optimal $NaY(Gd^{3+})(MoO_4)_2{:}Er^{3+}$ phosphors is higher than that of $CaLa_2(MoO_4)_4{:}Sm^{3+}/Eu^{3+}$ phosphors. The green emission intensity reduces minutely with the increasing of the temperature, which adequately indicates that the optimal $NaY(Gd^{3+})(MoO_4)_2{:}Er^{3+}$ phosphors may work at higher temperature and can be effectively applied to illumination, display and other practical applications. The thermal stability of the optimum sample is worthy to be favorable.

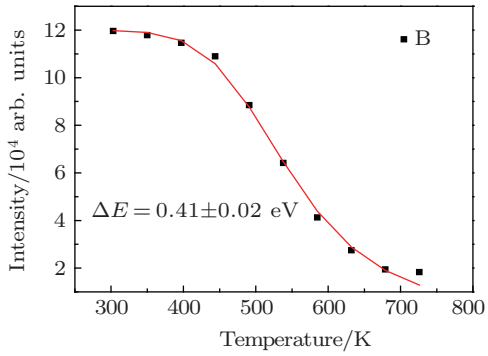



**Fig. 6.** (color online) Dependence of luminescence intensity on temperature.

## 4. Conclusions

The uniform design is used to obtain the doping concentration of rare earth ions with $Er^{3+}$[5.5%, 8.5%]$*Gd^{3+}$[60%, 90%]$*T$[700 °C, 1100 °C]. The three-factor orthogonal design of $Er^{3+}/Gd^{3+}/T$ and range analysis are employed to acquire the optimum combination of $Er^{3+}/Gd^{3+}/T$ with 5.5 mol%$Er^{3+}$, 70 mol%$Gd^{3+}$, and 1100 °C. The optimum $NaY(Gd^{3+})(MoO_4)_2{:}Er^{3+}$ phosphor with maximum green emission is synthesized by the high-temperature solid-state method. The XRD of optimum sample is characterized to verify its purity. Down-conversion excitation and emission spectra are also measured and the temperature effect on the optimum sample is analyzed according to the theory of the quenching temperature.

## References

[1] Jin Y, Zhang J H and Qin W P 2013 *J. Alloy. Compd.* **579** 263
[2] Zhang J P, Ma Z W, Han J B, Du G H, Zhou Y L, Liang L and Cheng Z 2013 *J. Lumin.* **144** 53
[3] Rambabu U, Munirathnam N R, Amalnerkar D P, PrakashT L, Reddy B S and Chatterjee S 2013 *Mater. Chem. Phys.* **142** 459
[4] Lu W L, Cheng L H, Zhong H Y, SunJ S, Wang J, Tian Y and Chen B J 2010 *J. Phys. D: Appl. Phys.* **43** 085404
[5] Santos P V, Araujo M T, Gouveia N A S, Neto J A M and Sombra A S B 1998 *Appl. Phys. Lett.* **73** 578
[6] Lu W L, Cheng L H, SunJ S, Zhong H Y Li X P, Tian Y, Wang J, Zhang Y F, Huang L B, Yu T T, Yu H Q and Chen B J 2010 *Physica B* **405** 3284
[7] Singh S K, Kumar K and Rai S B 2009 *Sensor Actuat. A: Phys.* **149** 16
[8] Zhao S L, Xu Z and Pei X J 2005 *Spectrosc. Spect. Anal.* **25** 1933
[9] Zhou D F, Shi C S, Zhang Q L and Chen Y H 2001 *Chin. J. Lumin.* **22** 248 (in Chinese)
[10] Ronda C R, Justel T and Nikol H 1998 *J. Alloy Compd.* **275** 669
[11] Xiao S, Yang X and Ding J W 2010 *Appl. Phys. B* **99** 769
[12] Tian Y, Qi X H, Wu X W, Hua R N and Chen B J 2009 *J. Phys. Chem. C* **113** 10767
[13] Taniguchi T, Soga K, Tokuzen K, Katsuya T, Takuro K, Koji T, Kenichi K, Nobuhiro M and Kiyoshi O 2012 *J. Mater. Sci.* **47** 2241
[14] Sun J Y, Cao C and Du H Y 2011 *Acta Phys. Sin.* **60** 127801 (in Chinese)
[15] Archilaa M A, Mandujanoa D G V, Cabrerab M A R, Lagunesb A G, M. SantillánbM, Cansecoa L M C, Micelia F A G and Dendoovenc L 2008 *J. Food Eng.* **84** 413
[16] Kackar R N, Lagergrcn E S and Filliben J J 1991 *J. Quality Technol.* **23** 107
[17] Liang Y Z, Fang K T and Xu Q S 2001 *Chemometr. Intell. Lab.* **58** 43
[18] Fang K T and Winker P 1998 *Technical Report MATH*-176, Hong Kong Baptist University
[19] Lee A W M, Chan W F, Yuen F S Y, Tse K P K, Liang Y Z and Fang K T 1997 *Chemometr. Intell. Lab.* **39** 11
[20] Lam L S, Chan W H, Leung C H and Luk C H 1998 *Chemometr. Intell. Lab.* **40** 203
[21] Hamid R, Yadollah Y, Ali E and Rezahajihosseini B 2008 *J. Chromatogr. A* **1196** 28
[22] Liu W, Li X L, Liu J, Han X, Yan J H, Kang Z H and Lian H Z 2011 *Acta Chim. Sin.* **69** 1565 (in Chinese)
[23] Pang M L, Lin J and Yu M 2004 *J. Solid State Chem.* **177** 2237
[24] Tao H, Bingham C M, Pilon D, Fan Kebin, Strikwerda A C, Shrekenhamer D and Padilla W J 2010 *J. Phys. D: Appl. Phys.* **43** 225102
[25] Zhai Z H, Sun J S, Zhang J S, Li X P, Cheng L H, Zhong H Y, Li J J and Chen B J 2013 *Acta Phys. Sin.* **62** 203301 (in Chinese)
[26] Cui W G, Li X H, Zhou S B and Weng J 2007 *J. Appl. Polym. Sci.* **103** 3105
[27] Zhang Y N, Yang S, Fan X N, Wang S, He N, Li L X, Luo D and Shi X M 2013 *Neural Regen. Res.* **8** 2641
[28] Tang Y S, Hu S F, Ke W, Lin C C, Bagkar N and Liu R 2008 *Appl. Phys. Lett.* **93** 131114
[29] Zhou T M, Zhang Y Q, Wu Z L and Chen B J 2015 *J. Rare Earth* **33** 686
[30] Zhong H, LiX P, Shen R S, Zhang J S, Sun J S, Zhong H Y, Cheng L H, Tian Y and Chen B J 2012 *J. Alloys Compd.* **517** 170
[31] Tian B N, Chen B J Tian Y, Li X P, Zhang J S, Sun J S, Zhong H Y, Cheng L H, Fu S B, Zhong H, Wang Y Z, Zhang X Q, Xia H P and Hua R N 2013 *J. Mater. Chem. C* **1** 2338